

Pyrolysis of superfine pulverized coal. Part 2. Mechanisms of carbon monoxide formation



Jiaxun Liu, Xiumin Jiang*, Jun Shen, Hai Zhang

School of Mechanical Engineering, Shanghai Jiao Tong University, Shanghai 200240, PR China

ARTICLE INFO

Article history:

Available online 4 August 2014

Keywords:

Superfine pulverized coal
Coal pyrolysis
CO formation mechanism
Curve deconvolution
CO₂ gasification

ABSTRACT

The oxygen-containing gases released during coal pyrolysis comprise more than a half of the devolatilization products, especially the noncondensable species. The mechanisms of CO formation reactions remain problematic, particularly the identity of the functional group precursors for low-temperature CO. In this paper, pyrolysis experiments of superfine pulverized coal were carried out in the N₂ and CO₂ atmosphere under non-isothermal conditions, applying a fixed-bed reactor. The CO formation mechanisms were investigated from a functional-group standpoint. The deconvolution method via numerical analysis was adopted to resolve the multi-component envelop profiles of CO evolution. Five constituent reaction complexes induced by different oxygenated groups and reactions are recognized, combining the X-ray photoelectron spectroscopy (XPS) analysis. In addition, the effects of coal type, particle size, pyrolysis atmosphere and heating rate on the CO evolution were analyzed. Finally, different CO formation mechanisms initiated from the primary decomposition of distinctive oxygenated functionalities, secondary pyrolysis reactions of tars, and gasification reactions of chars are summarized.

© 2014 Elsevier Ltd. All rights reserved.

1. Introduction

Coal pyrolysis is the initial step in all major coal utilization technologies, which has important influences on the subsequent thermochemical conversion processes, such as combustion, carbonization, gasification, and liquefaction [1,2]. The pyrolysis process also controls the characteristics of coal ignition, flame stability, fluidity, particle swelling, and soot formation, etc. [3,4]. The heterogeneous nature and complex components of coal make it difficult to fully interpret the coal pyrolysis mechanisms. Therefore, understanding coal pyrolysis is important to develop new coal utilization methods and pollution control strategies. It can also provide information about the heterogeneous components and physicochemical structures of coal.

The superfine pulverized coal (i.e., the average particle size around or below 20 μm) combustion technology has gained attention and credibility in recent years, because of the better flame stability, higher combustion efficiency and lower pollutant emission features, etc. [5–7]. During the devolatilization process, the evolving volatile products make remarkable changes in the chemical structure, surface morphology and porosity of the coal particles [5]. In addition, the gaseous products evolved from coal pyrolysis

such as aliphatic hydrocarbons, CO, and nitrogen precursors can alter the surrounding environment significantly [8]. Therefore, the understanding and description of volatile releasing characteristics during coal pyrolysis is important, especially the reducing species such as CH₄, CO and nitrogen precursors that can hinder the NO_x formation. Furthermore, preliminary studies indicate that with the decrease of coal particle sizes, the diffusion distance and resistance decreases, and the heat/mass transfer rate increases remarkably. It is interesting to note that superfine pulverized coal can promote the evolution of gaseous products during coal pyrolysis. The initial and maximum temperatures of the volatile evolution move forward, and the amounts of certain pyrolysis gases increase significantly, which is advantageous for the abatement of NO_x. Therefore, it is necessary to study the pyrolysis process of superfine pulverized coal. The mechanisms of CH₄ formation were discussed in the previous work, with data on CO evolution to be discussed here. The influences of coal particle sizes and atmospheres on the evolution of CO are focused in this publication.

It is important to obtain a more precise knowledge of the chemistry of coal pyrolysis, which is hampered by the heterogeneous nature and complex functional-group composition of coal. In spite of numerous works focused on the description of coal thermal decomposition, the mechanism of formation reactions for particular gaseous products of coal pyrolysis remains unclear. The formation of CO may originate from the decomposition of individual

* Corresponding author. Tel.: +86 21 3420 5681.

E-mail address: xiuminjiang@sjtu.edu.cn (X. Jiang).

functional groups, and secondary reactions of macromolecular network in coal. Seebauer et al. [9] studied the pyrolysis kinetics through thermogravimetric analysis (TGA), and revealed a sequence of three significant peaks of CO evolution curves. The secondary reactions played an important role in the formation of CO. Puente et al. [10] pointed out that CO₂ appears at lower temperatures than CO, which was originated from the decomposition of surface oxygen groups where C is bonded to one O atom. Arenillas et al. [11] suggested that CO occurred at different stages, which were originated from several oxygenated functions such as biaryl ethers and phenolic groups. Niksa [12] predicted the release of oxygen species using Flashchain theory. He suggested that the release of CO could involve low-temperature conversion of labile bridges and high-temperature decomposition of residual oxygen in nascent char links. Giroux et al. [13] attempted to relate oxygen-containing gases during coal pyrolysis to oxygenated functional groups. The results showed that the majority of CO was evolved at higher temperatures between 400 and 900 °C. Kelemen and Kwiatak [14] adopted X-ray photoelectron spectroscopy to determine organic oxygen species in reacted coal. The results showed that carboxyl and carbonyl groups were introduced during coal oxidation, which would produce CO during thermolysis. Hodek et al. [15] investigated the reactions of oxygen containing structures during coal pyrolysis. Three reaction steps with distinct temperature ranges were observed for CO releasing process. The different CO releasing mechanisms were attributed to the bond cleavage of aryl-methyl-ethers, biaryl-ethers, and condensed heterocyclic oxygen-containing structures.

In a word, CO is one of the major components of gas released during coal pyrolysis. The mechanisms of CO formation reactions remain problematic, particularly the identity of the functional group precursors for low-temperature CO [12,16]. There are few reports concerning the particle size effects on the CO evolution processes and pyrolysis mechanisms, not to mention the releasing processes from the superfine pulverized coal. In this paper, pyrolysis experiments of superfine pulverized coal were carried out under non-isothermal conditions, applying a fixed-bed reactor. The effects of coal type, particle size and atmosphere on the CO releasing mechanisms were analyzed. The deconvolution of the overall evolving curves was conducted through numerical analysis. The complex CO evolution curve profiles induced by a variety of chemical precursors were resolved. The individual component lines were assigned to different functional groups in the coal structure, based on the analysis of X-ray photoelectron spectroscopy (XPS).

2. Experimental section

2.1. Materials

Two typical Chinese coals studied in this work were Shenhua (SH) and Neimongol (NMG) bituminous coals with differences in maturation (i.e., the extent of coalification). The proximate and ultimate analyses are listed in Table 1. The coal samples were pulverized into different particle sizes using air jet mills. The particle size-distributions were collected by the Malvern MAM5004 Laser Mastersizer (Malvern, UK). The specific equivalent mean particle sizes of SH samples are 14.7, 17.4, 21.3 and 44.2 μm while NMG samples are 12.5, 14.9, 25.8 and 52.7 μm. The effect of temperature distribution within the sample particle can be eliminated during coal pyrolysis for such small particle sizes [17].

2.2. Apparatus and procedure

The coal pyrolysis experiments were performed at atmospheric pressure in a fixed-bed quartz reactor (electrically heated length

Table 1

Ultimate and proximate analysis of tested coal samples.

Proximate analysis (mass%) (ad)		Ultimate analysis (mass%) (ad)	
<i>SH</i>			
Moisture	11.5	C	63.13
Volatile	24.22	H	3.62
Ash	10.7	O	9.94
Fixed carbon	53.58	N	0.70
		S	0.41
<i>NMG</i>			
Moisture	14.72	C	54.82
Volatile	35.69	H	4.39
Ash	10.64	O	14.58
Fixed carbon	38.95	N	0.63
		S	0.22

ad – on an air dried basis.

O content is calculated by difference.

1000 mm with 28 mm inner diameter), which was depicted in the previous work [18]. About 0.4 g dry coal samples loaded in a porcelain boat were placed in the center of the reactor, where the temperatures were controlled by a programmed temperature controller, and measured precisely with a thermocouple. The coal samples were heated up to 800 °C at a constant heating rate of 10, 20, 30, or 35 °C/min. High-purity N₂ (>99.999%) or CO₂ (>99.999%) was used as the carrier gas with a flow rate of 3 L/min regulated by a mass flow controller. The gaseous products were analyzed on-line by a portable FTIR (Fourier transform infrared) gas analyzer Gasmet DX-4000 (Finland). The evolving products during coal pyrolysis including CH₄, CO, NH₃, NO, N₂O, NO₂, HCN, CO₂, SO₂, H₂O, HCl and HF can be measured quantitatively, with the lowest detectable concentrations of 0.1–2 ppm and the accuracy of 2%.

2.3. X-ray photoelectron spectroscopy (XPS) analysis method

The non-destructive technique of X-ray photoelectron spectroscopy (XPS) was adopted here for approximate quantification of organic functionalities in superfine pulverized coal. The XPS spectra were obtained on a PHI 5700 ESCA System with a hemispheric detector, using Al Kα nonmonochromatic radiation (1486.6 eV). All spectra were recorded at an analyzer-pass energy of 29.35 eV (narrow scan) and a constant analyzer transmission mode. An energy correction was made to account for sample charging based on the main carbon (1s) peak at 284.6 eV.

3. Results and discussions

3.1. Influences of coal rank and particle size on the CO formation mechanisms

Fig. 1 presents the CO evolution profiles of SH and NMG during coal pyrolysis in N₂ atmosphere. The fixed-bed reactor was heated from the room temperature up to 800 °C at a stable heating rate of 20 °C/min. A very broad thermal evolution profile of CO extended from around 200 °C to about 800 °C suggests a variety of chemical precursors and pyrolysis mechanisms. A sequence of three significant peaks is revealed for all coal samples, which is attributed to the multi-component structure with several superimposed peaks [19]. The presence of several oxygen-containing functionalities evolved at different temperatures induces the complex CO evolution curves. The distinctive temperature ranges of the degradation of heterogeneous complexes in various stages overlap each other, which causes the wide distribution of the overall CO evolution. The major proportion is generated within 600–800 °C, with the main peak occurring at around 700 °C [20].

The influence of coal rank on the evolution of CO can be observed in Fig. 1. The CO profile for the lower-rank NMG coals increases

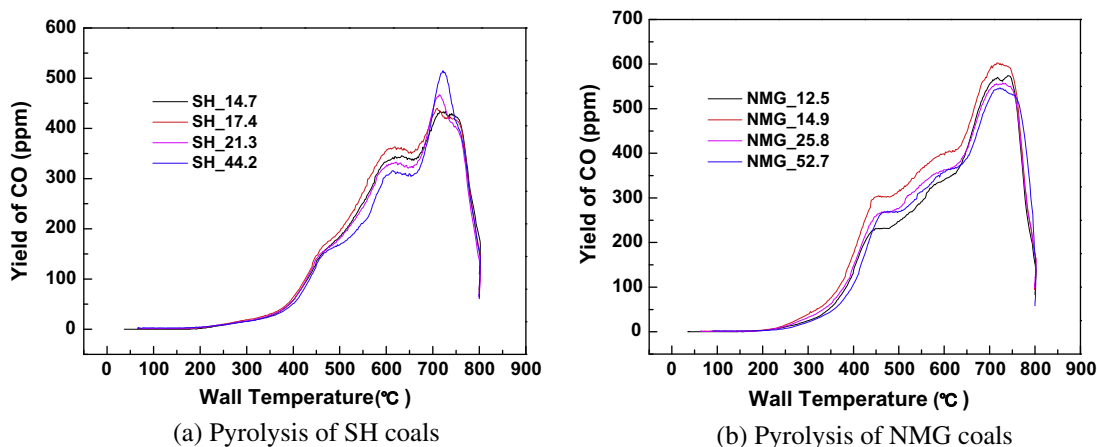


Fig. 1. Evolution of CO during coal pyrolysis in the N_2 atmosphere (heating rates $20\text{ }^\circ\text{C/min}$, temperature $800\text{ }^\circ\text{C}$, N_2 atmosphere).

evidently in magnitude compared to SH coals. The CO generation during coal pyrolysis decreases as the coal rank increases. Generally, the evolution of CO is attributed to the decomposition of oxygen functional groups in coal such as phenol, ether, ketone, quinone, carbonyl, methoxyl groups, and oxygen-containing heterocyclic structures, where C is bonded to one O atom [10,21]. A decreasing trend in oxygen content in coal is indicated from the elemental analysis, as the rank increases. It is consistent with the results from other analytical methods (e.g. XPS and ^{13}C NMR), which indicates the lost of carboxyl, hydroxyl, carbonyl, methoxyl groups etc. with increasing coalification [22,23]. Therefore, the amounts of CO evolved during pyrolysis of NMG coals are all higher than those from SH coals. During coal combustion, CO plays an important role in reducing NO_x , which makes the lower-rank coals more advantageous for the NO_x abatement.

Fig. 1 also reflects the influence of coal particle size on the CO evolution profiles. No significant differences in the lineshapes are found between the different particle sizes. A similar distribution of three significant peaks is revealed for all the fractions, which indicates the coal particle sizes have no significant effects on the reaction types and formation mechanisms on the CO evolution. On the other hand, a closer examination of the evolved curves shows the total yields of CO increase with decreasing particle sizes. This is related to the physiochemical properties of the superfine pulverized coal. Firstly, studies concluded that the singly-bonded oxygen substituents preferentially attacked on aliphatic structures. The carbonyl, carboxyl and phenolic groups could be formed at the expense of aliphatic and aromatic hydrogen at low temperatures [24–26]. During the superfine grinding processes in a jet mill, the huge energy intensity exerted on the coal particles may result in a mechanochemical effect [27]. All the comminution processes were performed in the ambient environment. Therefore, it is possible that certain components react with the oxygen in the atmosphere, leading to the increase of the oxygen functionalities in coals. The increased singly-bonded oxygen substituent in smaller coals causes the higher values of CO yields. Secondly, the specific surface areas and pore volumes increase significantly with the decrease of particle size. In the secondary pyrolysis reactions, the tar fractions are cracked during transport in the pores, inducing the formation of light gases like CO and methane [9]. Therefore, the instantaneous formation rate of CO inside the particle increases, which promotes the release of CO from smaller coal samples.

However, a critical particle size d_c exists around $15\text{ }\mu\text{m}$ ($14.9\text{ }\mu\text{m}$ for NMG coals, $17.4\text{ }\mu\text{m}$ for SH coals), where the largest amounts of CO are released. Hence, the lower-rank superfine pulverized coals

with the critical particle sizes take more advantage for inhibiting the NO_x formation. On the other hand, chemical reactions as well as physical changes are important for pyrolysis [28]. With further decreases in the particle sizes, the intraparticle mass concentration and temperature gradients are diminished. The release distance of pyrolytic products is shortened [29], and the holdup of volatiles within the particle is reduced. The resident time of larger pyrolysis fractions and small gaseous sources for CO is decreased. Most of these fragments are released before the secondary pyrolysis reactions even happen. Thus, the formation of CO is retarded, and the total yield is reduced.

3.2. Multi-component analysis of the CO formation mechanisms

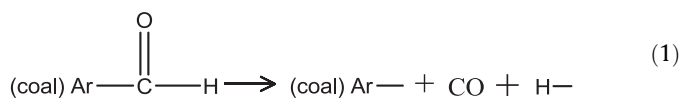
Coal has a complex and heterogeneous structure, which is generally accepted as a three-dimensional macromolecular network cross-linked by short aliphatic and etheric bridges. Abundant functional groups e.g. phenolic hydroxyl, ether, and alkyl side chains are substituted on the aromatic rings [30,31]. The formation of light gas species during coal pyrolysis is generally related to the decomposition of individual functional groups. The heterogeneity and variability of coal induces the complex character of the pyrolysis behaviors. The complicated profiles of the overall CO evolution, with a broad thermal distribution, suggest a variety of chemical precursors and component reactions are involved. However, the roles of individual groups in CO evolution processes are not well known so far, especially the identification of the specific functional-group precursors for low-temperature CO. In this paper, the deconvolution method through numerical analysis was adopted to resolve the multi-component evolving curves of CO. After the resolution of the overlapped profiles, the individual component lines were assigned to the specific oxygen-containing species through XPS analysis. The behaviors of different functionalities contributing to the individual component lines were further investigated based on the temperature positions. Finally, the CO formation mechanisms were concluded from a functional-group standpoint.

Each inflexion on the envelop evolution curve of CO during coal pyrolysis corresponds to a separate reaction, which is assumed to be characterized by specified kinetic parameters [32]. The distinctive temperature ranges of the degradation of heterogeneous sources in various stages overlap each other, which causes the complex wide evolution curves of CO. A different number ranged from three to five separate reactions has been suggested for the formation of CO [9,13,15]. It is observed from Fig. 1 that the overall evolution curve of CO formation can be characterized by three clearly visible peaks as well as two points of inflexion, located on

initial rising section (around 350 °C) and final falling part (around 760 °C). The visual inspection indicates that CO is formed as a result of five constituent reactions, which can be validated by the curve resolution. Two to six independent reaction complexes were introduced to simulate the CO generation trends, varying in peak parameters like the locations, linewidths, and intensities. The approximations of the experimental curves by the superposition of five Gaussian lines were considered as the best fitting results, which gave the highest correlation coefficients (i.e., the smallest values of the root mean square deviation). The multi-component structures of CO evolution rates of SH_14.7 and NMG_14.9 coals in N₂ atmosphere are shown in Fig. 2 (other particle sizes with similar results are not presented). The correlation coefficients of the lines are all greater than 0.99, which can be considered the validity of the simulation is preferable.

The decomposition of functional groups during coal pyrolysis is induced by the bond breaking and side-chain splitting. The functional groups with different bond dissociation energy result in the distinctive degradation temperature ranges during thermal cleavage. The temperatures of the maximum CO evolution rate (T_{\max}) of individual reaction complexes are summarized in Table 2. Generally, the T_{\max} of the SH coals are higher than those of the corresponding NMG coals. The constituent peak temperatures gradually shift to higher ranges with increasing coal ranks. The NMG coals with lower maturity are more abundant in oxygen functional groups. The various oxygenated precursors lead to the yields of CO etc. in the distinctive temperature zones, once the thermal degradation begins. Thus, with more available reacting agents, the instantaneous formation rate of CO inside the particle increases, which promotes the release of CO in lower ranking coals. In addition, it is interesting to note that similar trends are observed among different particle sizes. The peak temperatures are heightened with increasing the particle sizes. The evolution rates of the pyrolysis products depend on the concentration of the reacting agent, the kinetic parameters and the resident time [9]. Similarly, the abundant reacting agent of the oxygenated functionalities in smaller coal particles is one reason. This is because previous research indicates that the functional groups in superfine pulverized coal especially oxygen containing species increase with the decrease of particle sizes [18]. Additionally, the reaction kinetics can also induce the prompt release of CO from smaller coal particles. With the decrease of the particle sizes, the release distance of pyrolytic products is shortened, which lowers the mass transfer resistance. Also, the heat transfer rate is enhanced with the intraparticle thermal gradient being diminished in smaller particles. Therefore, the individual peak temperatures of CO evolution from larger particle fractions are basically higher than the smaller fractions.

The evolution process of CO can be divided into four stages, as shown in Fig. 2. There is a reaction step in extra low temperature ranges (below 350 °C) for all the coals. A minor peak centered around 300 °C is evident, and it decreases in magnitude as coal rank increases. In this first stage, loosely bonded precursors are eliminated first. The aldehyde groups that are weakly bonded to the matrix are the main sources of this minor feature. Based on the vibration strength analysis, the thermal stabilities of functional groups in coal are displayed as the following order: OH > —O— > C—H \approx aliphatic C—H > substituted aromatic ring > C=O > COOH > CHO [33,34]. The aldehyde group is the most active species in the coal molecular [34], which will be depleted in extra low temperature ranges, accompanied by the evolution of CO. The stage one can be simulated by one constituent reaction, peak I. The reaction type I is related to the loosely bonded aldehyde groups in coal, which are susceptible to be eliminated upon the treatment at temperatures above 200 °C, and released in the form of CO. A large number of hydrogen free radical is also produced, which plays an important role in the subsequent pyrolysis processes.



The stage two is assigned to the temperature range between 350 and 550 °C, where a large quantity of CO begins to release around 400 °C, followed by a steep increase trend, and reaches the maximum at about 450 °C. The reaction type II is attributed to the decomposition of carbonyl groups in coal, which are susceptible to be broken at low temperatures. The XPS analysis was applied to testify the validity of the carbonyl decomposition mechanism of CO. The curve fitting method was applied to resolve the multi-component XPS carbon (1s) spectra [34]. All the total curves could be best fitted by five mixed Gaussian–Lorentzian lines according to the binding energy of distinctive bonds in coal, which makes all the correlation coefficients higher than 0.99.

The multi-component structures of XPS spectra of NMG coals are reflected in Fig. 3. The 284.4 ± 0.3 eV peak corresponds to the aromatic and aliphatic carbon (C—C), while the 285.0 ± 0.3 eV peak generally represents C—H bonds. The 286.1 ± 0.2 eV peak has contributions mainly from the carbon single bonded to one oxygen (C—O e.g., ether and hydroxyl groups). The binding energy of 287.6 ± 0.3 eV is assigned to the carbon bound to oxygen by two bonds (C=O i.e., carbonyl). The 288.6 ± 0.4 eV peak is associated with the carbon bound to oxygen by three bonds (O—C=O, mainly carboxyl). The concentrations of the specific functional groups from XPS analysis are represented by the integrated areas of the

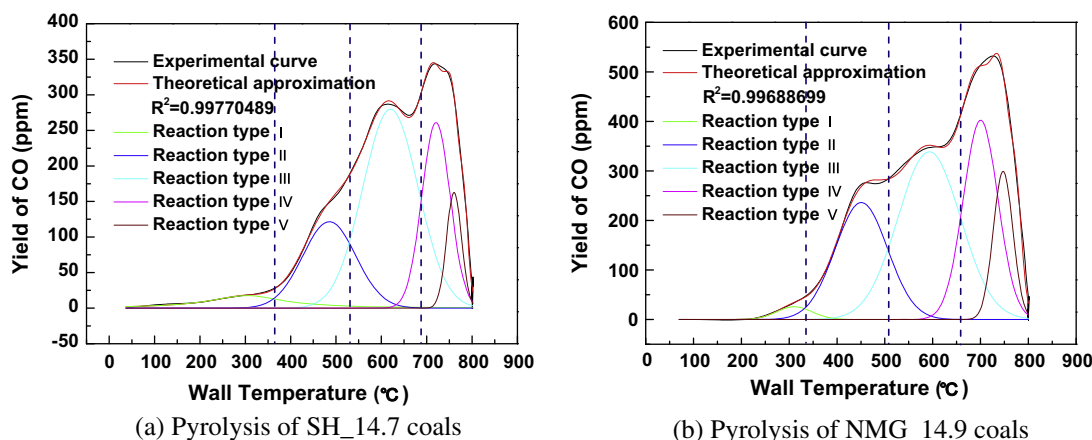
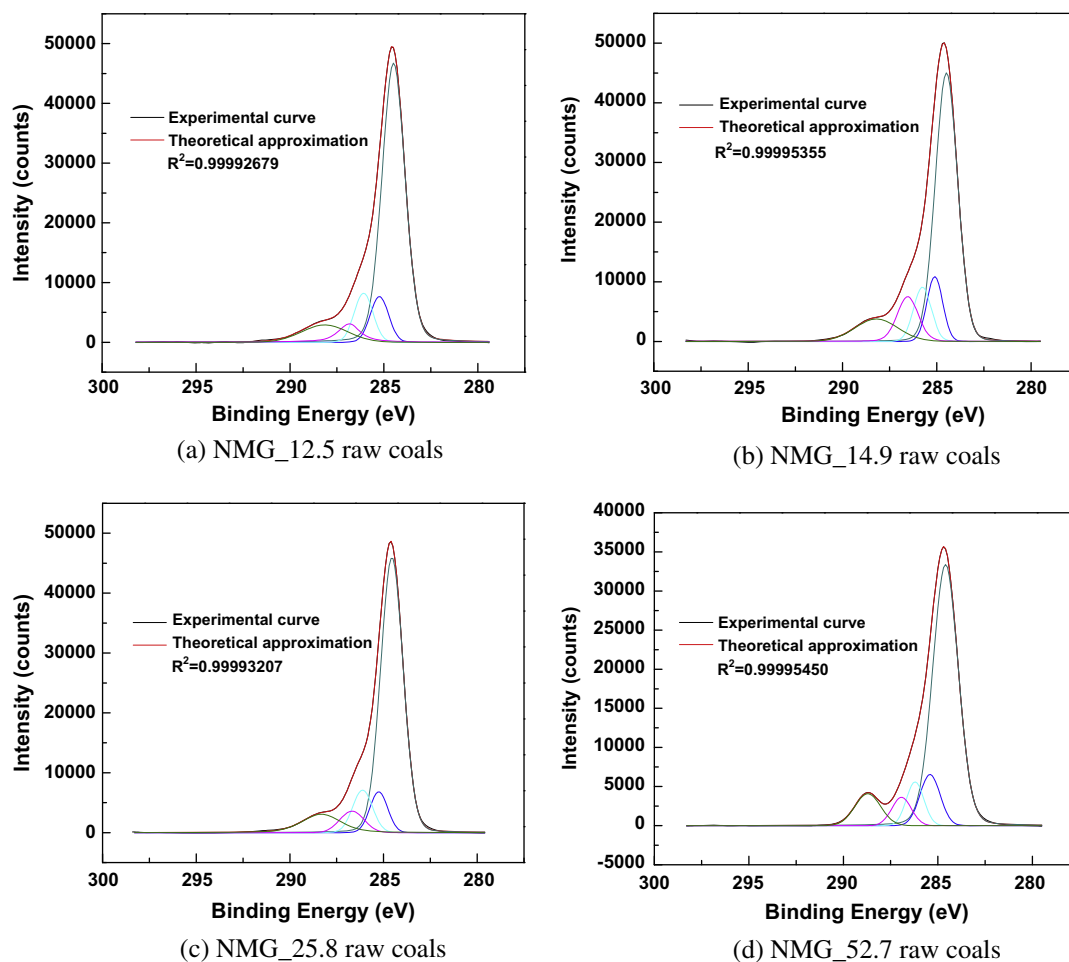


Fig. 2. Multi-component structure of CO evolution rates during pyrolysis in the N₂ atmosphere (heating rates 20 °C/min, temperature 800 °C, N₂ atmosphere).

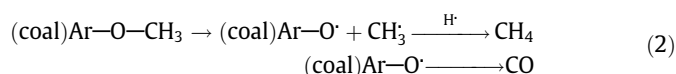
Table 2Temperatures of the maximum CO evolution rate of the constituent reactions (T_{\max} , heating rates 20 °C/min, temperature 800 °C, N₂ atmosphere).

Samples	Peak II (°C)	Peak III (°C)	Peak IV (°C)	Peak V (°C)	Proportion of peak III (% Area)
SH_14.7	477.76	618.69	721.41	764.03	48.49
SH_17.4	478.87	616.39	719.21	764.98	49.48
SH_21.3	485.21	618.16	720.07	767.17	45.10
SH_44.2	484.49	623.82	725.74	771.61	43.05
NMG_12.5	450.22	599.36	704.01	754.63	47.13
NMG_14.9	456.96	602.09	705.08	755.08	38.89
NMG_25.8	463.05	605.81	706.87	756.70	34.54
NMG_52.7	481.36	626.76	720.77	768.88	28.27

**Fig. 3.** Multi-component structures of C1s XPS spectra of NMG coal samples.

individual peaks, which are summarized in Table 3. The yields of CO from different stages are also listed there for comparison. It illustrates that the amounts of reaction-type-II CO are positively correlated to the concentrations of carbonyl functionalities. This indicates that the carbonyl groups are the precursors for the constituent peak II of the CO evolution.

Furthermore, the methoxyl groups in coal may enhance the CO evolution in this low temperature range. Plus, the demethylation of methoxyl groups is considered as an important source for the methane released at low temperatures. This explains the simultaneous occurrence of methane generation in the similar temperature range (300–500 °C), as expressed in the Eq. (2). Therefore, the methoxyl groups are also one of the precursors of the CO evolution.



The stage three contributes to the main part of the CO generation, which belongs to the temperature range of 550–700 °C. The proportions of constituent peak III account for up to 50% of the total CO yields, which are listed in Table 2. The cracking of tars during secondary pyrolysis reactions is believed to be the major source of this type of CO. The evaporation of the small fractions at low temperatures gives rise to the tar evolution during thermal degradation, when the bridge-breaking processes are predominant over the cross-linking reactions. The main tar-generation reactions take place around 450 °C, resulting in an intense release of the small and medium-sized clusters. Some of these condensable pyrolysis products are trapped in the pore structures of coal, with abundant oxygen being shuttled in the linkages in tar molecules (i.e., tar-O structures) [12]. Therefore, the decomposition of these tar-O structures leads to a rapid release of CO around 600 °C, when the tar evolution ceases. Niksa and co-workers [12,35] draw the similar

Table 3Relationships between CO reaction type and coal structures from XPS analysis (heating rates 20 °C/min, temperature 800 °C, N₂ atmosphere).

Samples	Reaction type II (area)	Carbonyl groups (area)	Reaction type IV + V (area)	Hydroxyl and Ether groups (area)
NMG_12.5	27109.24	6144.31	51485.80	10226.87
NMG_14.9	42357.15	11157.12	52152.78	10753.20
NMG_25.8	39076.17	5788.58	47401.17	9413.29
NMG_52.7	36837.73	4709.02	45950.42	6484.95

conclusion that there was a surge of CO evolution after the end of the tar formation, which was due to the secondary volatiles pyrolysis.

Furthermore, it is interesting to notice that the slopes of the envelop CO evolution curves of SH coals during the stage three are all larger than those of NMG coals. Hence, the increasing rate of the CO yields from reaction type III is larger for coals with higher maturity. This is because the CO formation mechanism of the stage three is mainly attributed to the secondary pyrolysis reactions, which has a close relationship with coal pore structures. The tar species can be converted to light gas when they are hindered in the pores of coal particles during the escape process. Our previous work shows that there is an apparent contraction of the pore structures with the coal rank especially on the small scale ones [36]. It can be clearly observed from Table 4 that SH coals have more small pores and higher BET specific surface (S_{BET}), which provides more active sites and reaction areas. The more complex pore network in higher ranking coals is advantageous for the tar degradation via secondary cracking reactions. Thus, the instantaneous formation rate of CO inside the particle increases in higher ranking coals, and the release of CO is more prompt.

The stage four accounts to the formation of CO after 700 °C, which contains two reaction complexes, peak IV and V. The hydroxyl groups with high bonding energies are responsible for the release of this late CO. For example, CO is split off through the reactions of the methyl and methylene radicals with the phenolic oxygen [15]. Furthermore, the ether groups in the residual char links are also recognized as the CO precursor during the stage four. The ether linkages can be formed through the condensation reactions between phenolic hydroxyls. CO can be released from the residual oxygen in nascent char links at high temperatures [12]. The relationship between the constituent peak IV and V and the concentrations of the ether and hydroxyl groups through XPS analysis are represented in Table 3. It elucidates that the amounts of the stage-four CO are positively correlated to the concentrations of the C–O groups in coal. Therefore, the ether and hydroxyl functionalities are the precursors for the high-temperature CO evolution during coal pyrolysis. In addition, the cleavage of heterocyclic oxygen-containing structures might also contribute to the release of this late CO [11,23,28]. These structures split off CO only at high temperatures (≈ 700 °C) [15].

In this work, thermogravimetric analysis (TGA) methods were applied to investigate the thermal behaviors coals on the Q600 simultaneous DSC-TGA (America). The detailed operational

parameters were described in the previous work. The relationships between the weight loss and corresponding temperatures were recorded.

The influence of particle size on the mass loss during coal pyrolysis (N₂ atmosphere, heating rates 20 °C/min.) was investigated through TGA analysis, shown in Fig. 4. Three separated peaks can be observed, which divide the pyrolysis process into three main stages. In this work, we mainly focus on the third peak around 700 °C, which coincides with the fourth stage of the CO evolution process. The release of the high-temperature CO contributes a lot to the weight loss of this stage. Other contents released during this same temperature range such as NH₃ (about 9 ppm) and HCN (about 5 ppm) are very small (see Fig. 5), which can be ignored compared to CO.

It can be observed from the magnified pictures in Fig. 4 that the mass loss rate of DTG curve around 700 °C shifts toward lower ranges, which indicates the release of high-temperature CO becomes more promptly and intensely for smaller coal particles. On the other hand, the maximum mass loss rate of this range shows different trends for NMG and SH coals. With the increase of the particle size, the mass loss rate decreases for NMG coals, while the opposite tendency is observed for SH coals. This is related to the contents of high-temperature CO precursors in parent coal, as shown in Fig. 6. The hydroxyl and ether groups that are the main sources of the high-temperature CO are higher in smaller NMG coals while larger SH coals are abundant with those groups. Therefore, it can be observed that more high-temperature CO is released for smaller fractions of NMG coals, while larger SH coal particles show higher yields of the fourth stage CO. We can draw the conclusion that the release of high-temperature CO leads to the mass loss of the third peak of DTG curve.

3.3. Influence of pyrolysis atmosphere on the CO formation mechanisms

CO₂ affects the coal pyrolysis significantly because CO₂ is a product and a reactant during coal degradation [37]. Especially, the gasification reaction between CO₂ and the char has notable influence on the CO evolution. Therefore, pyrolysis studies in CO₂ atmosphere need to be accomplished for better understanding of the CO formation mechanisms.

The evolution profiles of CO during SH and NMG coal pyrolysis in CO₂ atmosphere are reflected in Fig. 7. The temperatures were raised from the ambient temperature up to 800 °C at stable heating

Table 4

Conventional textural characteristics of tested coal samples.

Coal samples	Mean particle diameter (μm)	Mean pore diameter (nm)	S_{Lang} (m^2/g)	S_{BET} (m^2/g)	Pore volume (cm^3/g)
SH	14.7	9.4583	10.4151	7.1982	0.016787
	17.4	10.4997	10.1317	6.9808	0.017147
	21.3	13.8426	8.7381	6.1132	0.012262
	44.2	11.6307	8.9806	6.2866	0.012152
NMG	12.5	17.3606	12.3376	8.5623	0.036572
	14.9	17.7483	10.1676	6.9802	0.030057
	25.8	21.9093	8.1130	5.6349	0.028244
	52.7	20.7158	8.0251	5.4638	0.02344

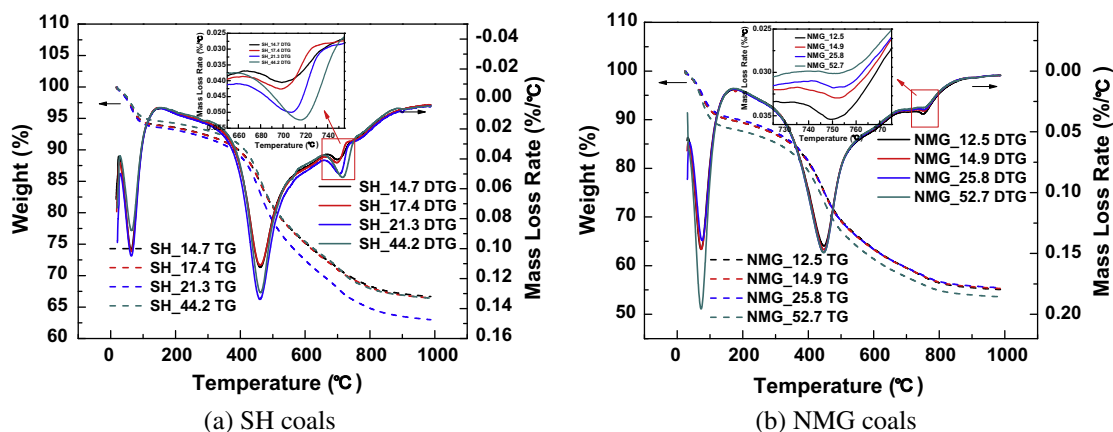


Fig. 4. TG/DTG curves of coal samples with different particle sizes (heating rates 20 °C/min, temperature 1000 °C, N₂ atmosphere).

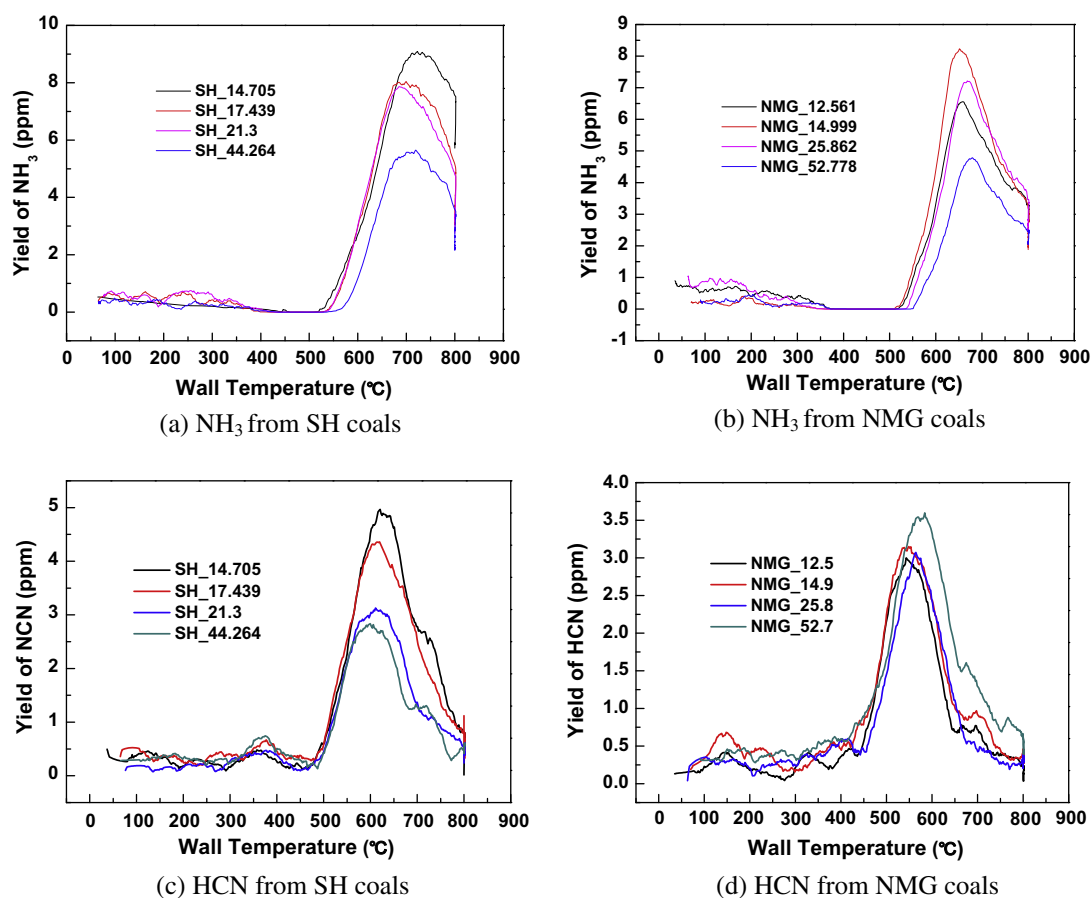


Fig. 5. Evolution of NH₃ and HCN during pyrolysis of coals in the N₂ atmosphere (heating rates 20 °C/min, temperature 800 °C, N₂ atmosphere).

rates of 20 °C/min. The CO formation curves of the CO₂ atmosphere show significant differences from N₂. During pyrolysis in the N₂ atmosphere, CO increases firstly with the increasing the temperatures, and decline promptly after it reaches the maximum around 710 °C. However, the total yields of CO show a monotonic increasing trend with the increase of temperatures during the whole pyrolysis process in the CO₂ atmosphere. The releasing process can be generally divided into two stages. Firstly, there is a slow increase of the CO formation before 520 °C. Then, the evolution of CO rises rapidly and increases monotonically afterward.

A tremendous difference of the CO yields exists between the two pyrolysis atmospheres. The amounts of CO released in the N₂

atmosphere are several tenths of those from the CO₂ atmosphere, which is mainly attributed to the gasification reactions between CO₂ and the chars. The differences in the evolution processes of CO are further compared in the magnified pictures in Fig. 7. It can be observed that in lower temperature ranges, there is only a slight difference between N₂ and CO₂ atmospheres. However, when the temperature reaches around 550 °C, the gasification reactions initiate the sharp increase of CO in the CO₂ atmosphere. Then, the disparities between the two atmospheres are widening. The corresponding temperature of the point of separation can be loosely taken as the onset temperature of the gasification reaction during coal pyrolysis process.

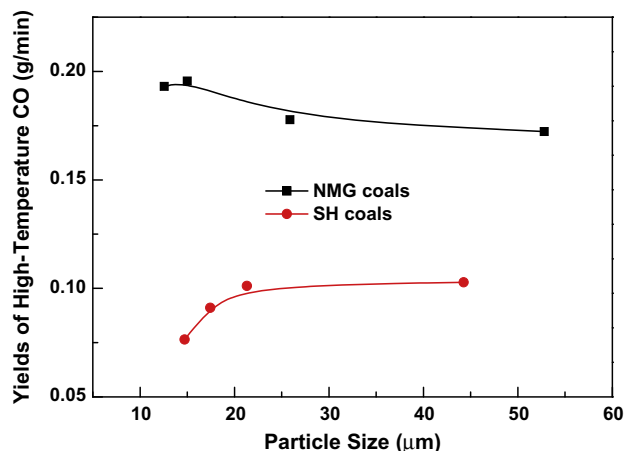


Fig. 6. Influence of particle size on the yields of high-temperature CO during coal pyrolysis in the N₂ atmosphere (heating rates 20 °C/min, temperature 800 °C, N₂ atmosphere).

Fig. 7 also elucidates the influence of coal rank on the CO evolution during coal pyrolysis in the CO₂ atmosphere. Much more CO is released from NMG coals compared to those from SH samples. It can be concluded that the yields of CO decrease with increasing coal maturities during pyrolysis in the CO₂ atmosphere. As mentioned before, the abundant reacting agent of the oxygenated functionalities in lower-rank coals is one reason. Furthermore, lower ranking coals with higher volatile contents result in the higher apparent char reactivity. In addition, coals with lower maturity have more larger pore structures (mesopores and macropores), which serve as the channels for reactant gas transportation. This can be observed from Table 4 that all the mean pore diameters of NMG coals are larger than SH coals. Therefore, the mass transfer resistance lowers down for the gas transportation, leading to the increase of the gasification reaction rate in NMG coals.

The effects of particle sizes on the yields of CO during coal pyrolysis in the CO₂ atmosphere are presented in Fig. 8. Basically, the amounts of CO show an increasing trend with the decrease of the particle sizes, especially for NMG coals. For SH coals, a similar tendency is observed as pyrolyzed in the N₂ atmosphere that a critical particle size d_c exists (SH_{17.4}), which releases the largest amounts of CO. However, the CO formation mechanisms are quite different for the CO₂ and N₂ atmospheres. The gasification reaction has significant influence on the yields of CO during coal pyrolysis in

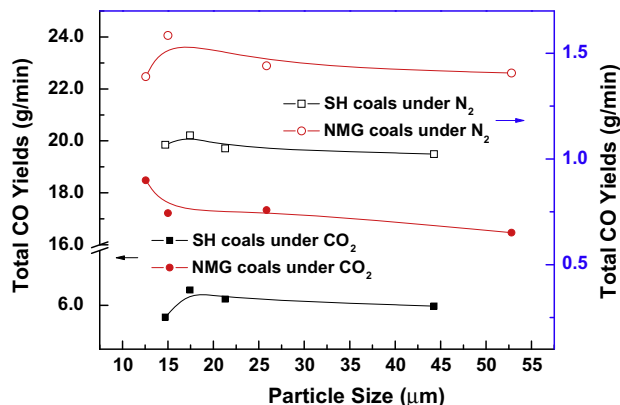
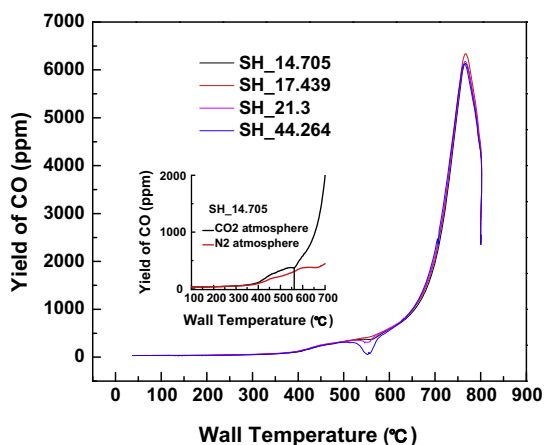
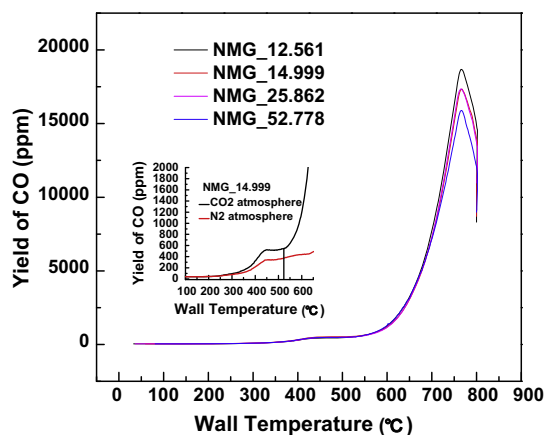


Fig. 8. Influence of particle size on the yield of CO during coal pyrolysis in different atmospheres (heating rates 20 °C/min, temperature 800 °C, N₂ and CO₂ atmosphere).

the CO₂ atmosphere. The pore structures play a crucial role in the gasification process that mainly includes the gaseous diffusion (internal and external diffusion) and surface reaction process. There are three steps in the surface reaction procedure. Firstly, the gaseous molecules produced during thermal decomposition are adsorbed on the inner pore surfaces in coal, leading to the formation of transient complexes. Then, the gasification products are evolved in the pores through the reactions between the gaseous molecules and complexes or among these complexes themselves. Eventually, the gasification products are conveyed to the exterior of the particles via the mass diffusion process. The pore networks of coal particles provide the reactive surfaces (micropores) and transportation channels for reactant gases (mesopores and macropores). Consequently, the pore characteristics in coal play a substantial role in the gasification processes. The evolution of CO from coal pyrolysis in the CO₂ atmosphere has a close relationship with the pore structures, which is displayed in Fig. 9. The pore volume distributions coincide with the CO yields, especially for NMG coals. Therefore, with the decrease of coal particles, more small pores in the matrix are exposed during the superfine comminution process, and the pore volume increases. Thus, the conclusion can be drawn that more CO is released from smaller coal particles with lower maturity, which is advantageous for the subsequent abatement of NO_x.



(a) Pyrolysis of SH coals



(b) Pyrolysis of NMG coals

Fig. 7. Evolution of CO during coal pyrolysis in the CO₂ atmosphere (heating rates 20 °C/min, temperature 800 °C, CO₂ atmosphere).

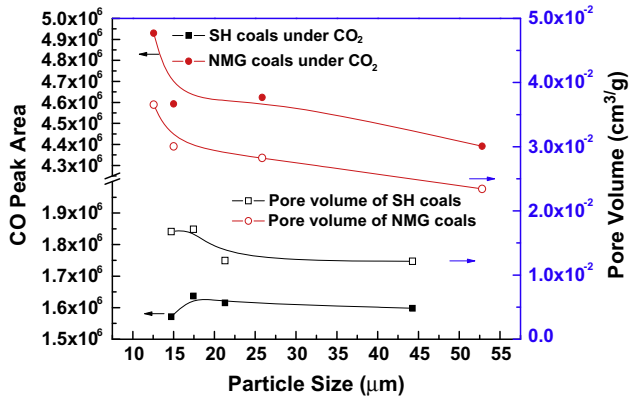


Fig. 9. Relationships between the pore volumes and the yields of CO during coal pyrolysis in the CO₂ atmosphere (heating rates 20 °C/min, temperature 800 °C, CO₂ atmosphere).

3.4. Influence of heating rate on the CO formation mechanism

Experiments were carried out to study the influence of heating rate on the CO evolution during coal pyrolysis in N₂ and CO₂ atmospheres. The coal samples were heated up to 600 °C at different heating rates of 10, 20, 30, and 35 °C/min. The typical CO evolution curves of SH_{14.7} in different atmospheres are shown in Fig. 10. With the increase of the heating rates, the ultimate yields of CO in N₂ and CO₂ atmospheres both increase tremendously. Intraparticle secondary reactions contribute to the majority evolution of CO in the N₂ atmosphere. The production of the tars that are available as reactant sources plays a crucial role in the CO evolution. The competing reactions between the evaporation and condensation of the small and medium sized clusters (i.e., tar precursors) determine the ultimate tar yields. Tar generation rather than tar polymerization is the dominant reactions at high heating rates, leading to the increase of tars [9]. Thus, the evolution of CO is accelerated because of the higher concentration of the reacting agents. On the other hand, it can be observed from Fig. 10 that the release of CO is susceptible to be saturated with further increasing the heating rates. The difference of CO yields between 30 and 35 °C/min is reducing, and the influence is weakening at higher heating rates. Less time is available at higher rates during the heating up process of coal. Shorter reaction time results in less tar cracking reactions to produce CO. Therefore, the growth of CO yields is slowing down at higher heating rates. It is the same reasons that a similar tendency is observed in the influence of

heating rates on the CO evolution from CO₂ pyrolysis. Heating rates have significant effects on the intermediate and transient complexes of the gasification reactions. Furthermore, the thermal lag phenomenon occurs during rapid surface heating [38], which retards the gasification reactions, and the onset temperatures shift toward higher zones.

It is worth noticing that there is an obvious concave valley around 550 °C on the CO evolution curve in the CO₂ atmosphere. This hollow may be related to the reduction of N₂O, which is presented as the small chart in Fig. 10 (b). The evolution of N₂O during coal pyrolysis in the CO₂ atmosphere shows a sharp decline in the same temperature ranges (around 550 °C). The strong chemical adsorption and desorption processes during gasification reactions promote the formation of new reactive sites on the char surfaces, e.g., $-(C)_{solid}$ and $-(CO)_{solid}$. Thus, N₂O can be homogeneously and heterogeneously reduced to N₂ with the participation of CO, as shown in the Eqs. (3)–(5) [5]. Correspondingly, there will be a prompt release of N₂ during this temperature ranges. Therefore, the large consumption of CO through chemical adsorption and homogeneous reduction causes the concave valley on the evolution profile.



A non-isothermal method developed by Kissinger [39] was applied in this work to obtain the kinetic parameters of the CO evolution. The release of CO through the decomposition of specific functional groups is assumed to be first order reaction. Then, the single first order model [40] can be applied to derive the kinetic parameters by recording the maximum CO evolution temperatures at different heating rates. The activation energy E and the pre-exponential factor k_0 can be calculated through the slope and the intercept of the line, which is concluded from a linear relationship between $\ln\left(\frac{\beta}{T_{max}^2}\right)$ and $1/T_{max}$ (see the Eq. (6)).

$$\ln\left(\frac{\beta}{T_{max}^2}\right) = -\frac{E}{RT_{max}} + \ln\left(\frac{k_0R}{E}\right) \quad (6)$$

where k_0 is the frequency factor or pre-exponential factor in s⁻¹; E represents the activation energy in (J mol⁻¹); R refers to the gas constant in (J mol⁻¹ K⁻¹); T_{max} is the maximum CO evolution temperature in K; β represents the constant heating rate in non-isothermal

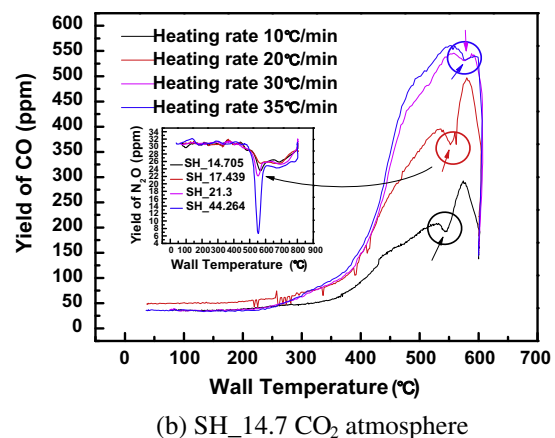
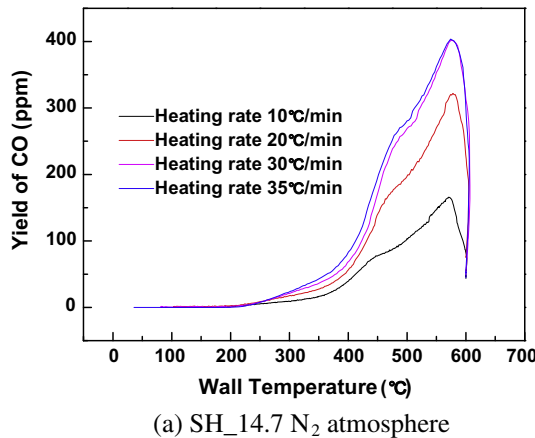


Fig. 10. Influence of heating rates on the evolution of CO (heating rates 10, 20, 30, and 35 °C/min, temperature 600 °C, N₂ and CO₂ atmospheres).

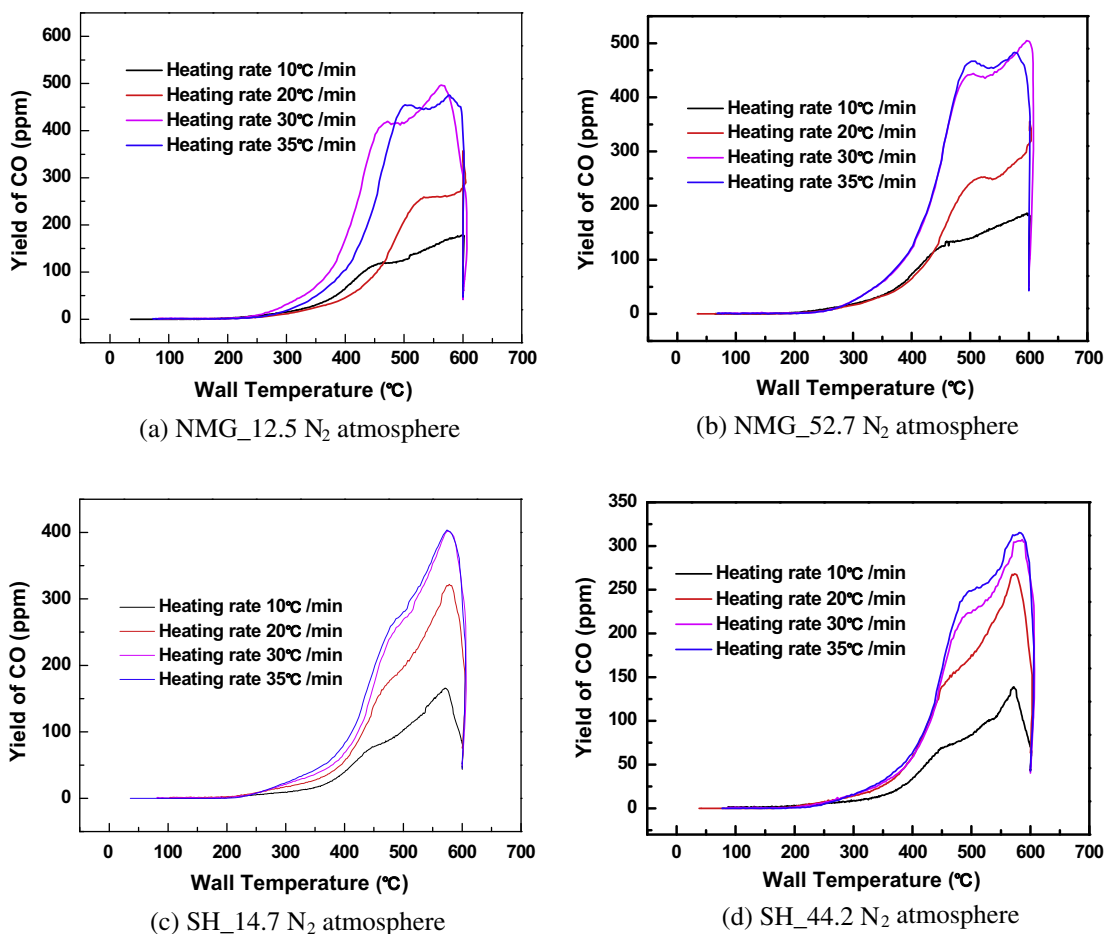


Fig. 11. Influence of heating rates on the evolution of CO (heating rates 10, 20, 30, and 35 °C/min, temperature 600 °C, N₂ atmosphere).

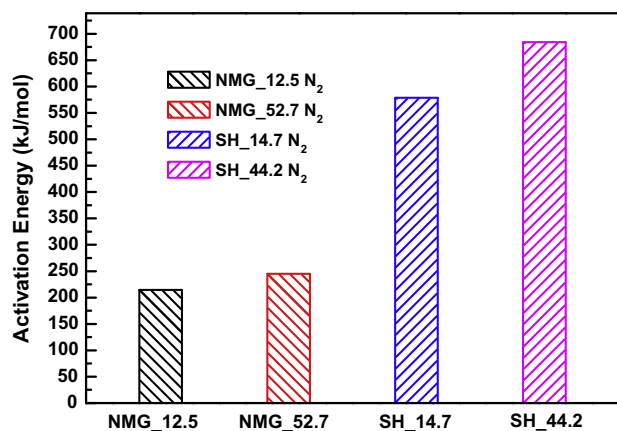


Fig. 12. Activation energies of CO evolution during coal pyrolysis in the N₂ atmosphere (heating rates 10, 20, 30, and 35 °C/min, temperature 600 °C, N₂ atmosphere).

experiments in (K min⁻¹). The detailed kinetic model descriptions are presented in Part 1.

Fig. 11 shows more typical CO evolution profiles during coal pyrolysis in the N₂ atmosphere at different heating rates of 10, 20, 30, and 35 °C/min. The maximum CO evolution temperature of each curve was concluded. Then, the activation energy of CO evolution during coal pyrolysis determined by the Eq. (6) is displayed in Fig. 12. The activation energies show a significant increase for SH

coal particles, which suggest that the release of CO is hard for high-maturity coals. This is in agreement with the observation from Fig. 1 that the amounts of CO for the higher-rank SH coals decrease significantly compared to NMG coals. Furthermore, the high values of E indicate that the release of CO is hard for SH coals, which can also be observed from Table 2 that the CO evolution gradually shifts to higher temperatures with increasing coal ranks. The different contents of oxygen functional groups in parent coals are the main reasons. There is an elimination of oxygen-containing structures groups like methoxyl groups during the coalification process, which is adverse to the evolution of CO. Similarly, it is noticed that the CO activation energies are higher for larger coal particles. The smaller the E is, the reaction rate is higher and the reactivity is better. Thus, the release of CO becomes easier and more prompt for smaller coals. The same conclusion is drawn from Table 2 that the peak temperatures are heightened with increasing the particle sizes, and the release of CO is retarded.

4. Conclusions

Based upon the investigations on CO formation mechanisms during superfine pulverized coal pyrolysis in the N₂ and CO₂ atmosphere, the following conclusions can be drawn:

1. The thermal evolution profile of CO during coal pyrolysis in the N₂ atmosphere extends broadly with a sequence of three significant peaks. The ultimate CO yield declines evidently as the coal rank increases. With the decrease of the particle sizes, the CO evolution increases. However, a critical particle size d_c exists around 15 μm , which releases the largest amounts of CO.

2. The evolution process of CO during coal pyrolysis in the N₂ atmosphere can be divided into four main stages, which are <350 °C, 350–550 °C, 550–700 °C and >700 °C, separately. The multi-component envelop evolving curves are resolved into five constituent reactions. The constituent peak temperatures gradually shift to higher ranges with the increase of coal ranks and particle sizes.
3. The reaction type I is related to the loosely bonded aldehyde groups in coal, which are depleted in extra low temperature ranges, and released in the form of CO. The constituent peak II of the CO evolution is attributed to the decomposition of carbonyl groups in coal, which is validated through XPS analysis. The reaction complex III is the major source of the CO generation, which is formed through the secondary pyrolysis reactions of tars. The ether and hydroxyl groups with high bonding energies are responsible for the release of the late CO after 700 °C.
4. The evolution of CO during coal pyrolysis in the CO₂ atmosphere shows a monotonic increasing trend with raising the temperatures. The ultimate yields of CO are tremendously enhanced by the gasification reactions between CO₂ and chars. The amounts of CO decrease with increasing coal maturities and particle sizes, which coincide with the pore volume distributions in coal.
5. With the increase of the heating rates, the evolution rates and total yields of CO in N₂ and CO₂ atmospheres both increase tremendously. However, the release of CO is susceptible to be saturated with further increasing the heating rates, and the growth of CO yields is slowing down. The gasification reactions are retarded due to the thermal lag effects at higher heating rates. The large consumption of CO through chemical adsorption and homogeneous reduction of N₂O causes the concave valley around 550 °C on the CO evolution curve in the CO₂ atmosphere.

Acknowledgements

This work was supported by the National Natural Science Foundation of China (Grant Nos. 51306116 and 51376131). The authors are grateful to the Instrumental Analysis Center of SJTU for giving the opportunity for the TGA experiments.

References

- [1] Aboyade AO, Carrier M, Meyer EL, Knoetze H, Görgens JF. Slow and pressurized co-pyrolysis of coal and agricultural residues. *Energy Convers Manage* 2013;65:198–207.
- [2] Ahmad T, Awan IA, Nisar J, Ahmad I. Influence of inherent minerals and pyrolysis temperature on the yield of pyrolysates of some Pakistani coals. *Energy Convers Manage* 2009;50:1163–71.
- [3] Solomon PR, Fletcher TH, Pugmire RJ. Progress in coal pyrolysis. *Fuel* 1993;72:587–97.
- [4] Solomon PR, Fletcher TH. Impact of coal pyrolysis on combustion. *Proc Combust Inst* 1994;25:463–74.
- [5] Liu JX, Gao S, Jiang XM, Shen J, Zhang H. NO emission characteristics of superfine pulverized coal combustion in the O₂/CO₂ atmosphere. *Energy Convers Manage* 2014;77:349–55.
- [6] Shen J, Liu JX, Zhang H, Jiang XM. NO_x emission characteristics of superfine pulverized anthracite coal in air-staged combustion. *Energy Convers Manage* 2013;74:454–61.
- [7] Zhang CQ, Jiang XM, Wei LH, Wang H. Research on pyrolysis characteristics and kinetics of super fine and conventional pulverized coal. *Energy Convers Manage* 2007;48:797–802.
- [8] Solomon PR, Serio MA, Suuberg EM. Coal pyrolysis: experiments, kinetic rates and mechanisms. *Prog Energy Combust Sci* 1992;18:133–220.
- [9] Seebauer V, Petek J, Staudinger G. Effects of particle size, heating rate and pressure on measurement of pyrolysis kinetics by thermogravimetric analysis. *Fuel* 1997;76:1277–82.
- [10] de la Puente G, Pis JJ, Menéndez JA, Grange P. Thermal stability of oxygenated carbons functions in activated. *J Anal Appl Pyrol* 1997;43:125–38.
- [11] Arenillas A, Rubiera F, Pis JJ, Cuesta MJ, Iglesias MJ, Jiménez A, et al. Thermal behaviour during the pyrolysis of low rank perhydrous coals. *J Anal Appl Pyrol* 2003;68–69:371–85.
- [12] Niksa S. Flashchain theory for rapid coal devolatilization kinetics. 7. Predicting the release of oxygen species from various coals. *Energy Fuels* 1996;10:173–87.
- [13] Giroux L, Charland JP, MacPhee JA. Application of thermogravimetric fourier transform infrared spectroscopy (TG-FTIR) to the analysis of oxygen functional groups in coal. *Energy Fuels* 2006;20:1988–96.
- [14] Kelemen SR, Kwiatek PJ. Quantification of organic oxygen species on the surface of fresh and reacted argonne premium coal. *Energy Fuel* 1996;9:841–8.
- [15] Hodek W, Kirschstein J, van Heek KH. Reactions of oxygen containing structures in coal pyrolysis. *Fuel* 1991;70:424–8.
- [16] Gaveau B, Letolle R, Monthieux M. Evaluation of kinetic parameters from ¹³C isotopic effect during coal pyrolysis. *Fuel* 1987;66:228–31.
- [17] Kok MV. Simultaneous thermogravimetry–calorimetry study on the combustion of coal samples: effect of heating rate. *Energy Convers Manage* 2012;53:40–4.
- [18] Liu JX, Jiang XM, Huang XY, Shen J, Wu SH. Investigation of the diffuse interfacial layer of superfine pulverized coal and char particles. *Energy Fuels* 2011;25:684–93.
- [19] Jüntgen H. Review of the kinetics of pyrolysis and hydropyrolysis in relation to the chemical constitution of coal. *Fuel* 1964;63:731–7.
- [20] Burnham AK, Oh MS, Crawford RW, Samoun AM. Pyrolysis of argonne premium coals: activation energy distributions and related chemistry. *Energy Fuels* 1989;3:42–55.
- [21] Siskin M, Scoutén CG. Sources of carbon dioxide formed during coal pyrolysis. *Energy Fuels* 1989;3:427–8.
- [22] Solum MS, Pugmire RJ, Grant DM. ¹³C Solid-state NMR of argonne premium coals. *Energy Fuels* 1989;3:187–93.
- [23] Kelemen SR, Afeworki M, Gorbaty ML, Cohen AD. Characterization of organically bound oxygen forms in Lignites, Peats, and pyrolyzed Peats by X-ray photoelectron spectroscopy (XPS) and solid-state ¹³C NMR methods. *Energy Fuels* 2002;16:1450–62.
- [24] Khan MR, Usman R, Newton E, Beer S, Chisholm W. E.s.r. spectroscopic study on the chemistry of coal oxidation. *Fuel* 1988;67:1668–73.
- [25] Swarm PD, Evans DG. Low-temperature oxidation of brown coal. 3. Reaction with molecular oxygen at temperatures close to ambient. *Fuel* 1979;58:276–80.
- [26] de la Puente G, Iglesias MJ, Fuente E, Pis JJ. Changes in the structure of coals of different rank due to oxidation-effects on pyrolysis behaviour. *J Anal Appl Pyrol* 1998;47:33–42.
- [27] Palaniandy S, Azizli KAM, Hussin H, Hashim SFS. Mechanochemistry of silica on jet milling. *J Mater Process Technol* 2008;205:119–27.
- [28] Ozbas KE. Effect of particle size on pyrolysis characteristics of Elbistan Lignite. *J Therm Anal Calorim* 2008;93:641–9.
- [29] Fan JJ, Zhang ZX, Jin J, Zhang JM. Investigation on the release characteristics of light hydrocarbon during pulverized coal pyrolysis. *Energy Fuels* 2007;21:2805–8.
- [30] Ndaji FE, Butterfield IM, Thomas KM. Changes in the macromolecular structure of coals with pyrolysis temperature. *Fuel* 1997;76:169–77.
- [31] Poutsma ML. Free-radical thermolysis and hydrogenolysis of model hydrocarbons relevant to processing of coal. *Energy Fuels* 1990;4:113–31.
- [32] Porada S. The reactions of formation of selected gas products during coal pyrolysis. *Fuel* 2004;83:1191–6.
- [33] Feng J, Li WY, Xie KC. Thermal decomposition behaviors of Lignite by pyrolysis-FTIR. *Energy Sources Part A* 2006;28:167–75.
- [34] Robert P, Helena W. The influence of oxidation with HNO₃ on the surface composition of high-sulphur coals XPS study. *Fuel Process Technol* 2006;87:1021–9.
- [35] Chen JC, Niksa S. Coal devolatilization during rapid transient heating. 1. Primary devolatilization. *Energy Fuels* 1992;6:254–64.
- [36] Liu JX, Jiang XM, Huang XY, Wu SH. Morphological characterization of super fine pulverized coal particle. Part 4. Nitrogen adsorption and small angle X-ray scattering study. *Energy Fuels* 2010;24:3072–85.
- [37] Duan LB, Zhao CS, Zhou W, Qu CR, Chen XP. Investigation on coal pyrolysis in CO₂ atmosphere. *Energy Fuels* 2009;23:3826–30.
- [38] Griffin TP, Howard JB, Peters WA. An experimental and modeling study of heating rate and particle size effects in bituminous coal pyrolysis. *Energy Fuels* 1993;7:291–305.
- [39] Kissinger HE. Reactive kinetics in differential thermal analysis. *Anal Chem* 1957;29:1702–6.
- [40] Holstein A, Bassilakis R, Wójtowicz MA, Serio MA. Kinetics of methane and tar evolution during coal pyrolysis. *Proc Combust Inst* 2005;30:2177–85.